2023

ESTABLISHING DEGRADATION OF THE C. ELEGANS DREAM COMPLEX IN THE GERMLINE

Christina M. Boody
Michigan Technological University, cmboody@mtu.edu

ESTABLISHING DEGRADATION OF THE *C. ELEGANS* DREAM COMPLEX IN THE GERMLINE

By

Christina M. Boody

A THESIS

Submitted in partial fulfillment of the requirements for the degree of

MASTER OF SCIENCE

In Biological Sciences

MICHIGAN TECHNOLOGICAL UNIVERSITY

2023

This thesis has been approved in partial fulfillment of the requirements for the Degree of MASTER OF SCIENCE in Biological Sciences.

Department of Biological Sciences

Thesis Advisor:	*Paul Goetsch*
Committee Member:	*Xiaohu Tang*
Committee Member:	*Zhiying Shan*
Department Chair:	*Casey Huckins*

Table of Contents

List of Figures iv

List of Tables v

Acknowledgements vi

Abstract vii

1 Introduction 1
- 1.1 The Eukaryotic Cell Cycle 1
  - 1.1.1 DREAM Complex 3
  - 1.1.2 Tissue-Specific Activity of DREAM 5
  - 1.1.3 Auxin-Inducible Degron System 6
  - 1.1.4 Study Hypothesis 8
- 1.2 Materials and Methods 13
  - 1.2.1 Worm Strains 13
  - 1.2.2 Worm Maintenance 13
  - 1.2.3 Brood Counting Experiments 13
  - 1.2.4 Dissection of *C. elegans* 14
  - 1.2.5 Fluorescent Imaging of the *C. elegans* germline 15
- 1.3 Results 15
  - 1.3.1 LIN-54 degradation in all cell types causes decreased brood size 15
  - 1.3.2 High lethality after auxin exposure in *eft-3*p-TIR1 transgenic strain with degron-tagged LIN-54 17
  - 1.3.3 LIN-35 Degradation in all cell types causes decreased brood size 18
- 1.4 Discussion 41

2 Reference List 43

List of Figures

Figure 1 DREAM complex in *C. elegans* 10

Figure 2 MuvB complex in *C. elegans* 11

Figure 3 The Auxin Inducible Degron System 12

Figure 4 *rps-28*p-TIR1 transgenic strain with degron-tagged LIN-54 brood counting experiment 22

Figure 5 *rps-28*p-TIR1 transgenic strain with degron-tagged LIN-54 Fluorescent Imaging 1 23

Figure 6 *rps-28*p-TIR1 transgenic strain with degron-tagged LIN-54 Fluorescent Imaging 2 24

Figure 7 *rps-28*p-TIR1 transgenic strain with degron-tagged LIN-54 Fluorescent Imaging 3 25

Figure 8 *eft-3*p-TIR1 transgenic strain with degron-tagged LIN-54 brood counting experiment 27

Figure 9 *eft-3*p-TIR1 transgenic strain with degron-tagged LIN-54 Fluorescent Imaging 1 28

Figure 10 *eft-3*p-TIR1 transgenic strain with degron-tagged LIN-54 Fluorescent Imaging 2… 29

Figure 11 *eft-3*p-TIR1 transgenic strain with degron-tagged LIN-54 Fluorescent Imaging 3… 30

Figure 12 *rps-28*p-TIR1 transgenic strain with degron-tagged LIN-35 brood counting experiment 32

Figure 13 *rps-28*p-TIR1 transgenic strain with degron-tagged LIN-35 Fluorescent Imaging 1 33

Figure 14 *rps-28*p-TIR1 transgenic strain with degron-tagged LIN-35 Fluorescent Imaging 2 34

Figure 15 *rps-28*p-TIR1 transgenic strain with degron-tagged LIN-35 Fluorescent Imaging 3 35

Figure 16 *eft-3*p-TIR1 transgenic strain with degron-tagged LIN-35 brood counting experiment 37

Figure 17 *eft-3*p-TIR1 transgenic strain with degron-tagged LIN-35 Fluorescent Imaging 1… 38

Figure 18 *eft-3*p-TIR1 transgenic strain with degron-tagged LIN-35 Fluorescent Imaging 2 39

Figure 19 *eft-3*p-TIR1 transgenic strain with degron-tagged LIN-35 Fluorescent Imaging 3 40

List of Tables

Table 1 Brood sizes of *rps-28*p-TIR1 transgenic strain with degron-tagged LIN-54… 21

Table 2 Brood sizes of *eft-3*p-TIR1 transgenic strain with degron-tagged LIN-54… 26

Table 3 Brood sizes of *rps-28*p-TIR1 transgenic strain with degron-tagged LIN-35… 31

Table 4 Brood Sizes of *eft-3*p-TIR1 transgenic strain with degron-tagged LIN-35… 36

Acknowledgements

I would like to express my deepest gratitude to my mentors, family, and friends. First, I want to say a massive “thank you!” to Dr. Paul Goetsch and PhD Candidate Emily Washeleski for guiding me through every step of this journey. I greatly appreciate the patience and encouragement you’ve shown me. Thank you to Dr. Xiaohu Tang and Dr. Zhiying Shan for enthusiastically volunteering to lend your expertise as members of my committee.

Dad, thank you for always supporting me and being the best dad ever. Mom, thank you for telling the funniest stories whenever I visited home. Helena, I know you will be happy I’ll have much more time for video games after this.

Lauren, thank you for always having something hilarious to say. I look forward to more adventures when I return home. Evan, thank you for constantly driving me home from the lab when I didn’t want to walk in the cold, and for listening to me talk endlessly about my research. You both rock.

Abstract

The highly conserved Dp, Rb, E2F, and MuvB (DREAM) complex is responsible for the transcriptional repression of cell cycle genes. The DREAM complex has been extensively studied in somatic (non-reproductive) cells, but there is a gap in knowledge regarding how the DREAM complex may function in germ (reproductive) cells. To demonstrate loss-of-function of DREAM in the germline, we used the auxin-inducible degron (AID) system to establish degradation of LIN-54, a subunit of DREAM's MuvB subcomplex, and the Retinoblastoma-like pocket protein LIN-35 in *C. elegans*. Using transgenic lines that express the *Arabidopsis thaliana* TIR1 E3 ubiquitin ligase ubiquitously through all *C. elegans* tissues or specifically only in somatic tissue, we evaluated the effects following treatment of auxin that triggers TIR1-mediated rapid degradation of degron-tagged LIN-54 or degron-tagged LIN-35. In our LIN-54 evaluation, brood size counting experiments showed a difference in fertility between worms exposed to auxin and the control group in both TIR1 transgenic lines, suggesting either that LIN-54's somatic activity is important for fertility or the somatic-expressed TIR1 transgene had some activity in the germline. Subsequent fluorescence microscopy revealed decreased expression of LIN-54 or LIN-35 in the germline in each TIR1-expressing transgenic worm background when exposed to auxin, as compared to the control group, indicating that the somatically-expressed TIR1 transgene does have activity in the germline. These results suggest that DREAM disruption in the germline negatively affects germ cell production and fertility. Our results underscore that new TIR1-expressing

transgenic lines will have to be generated to confirm that DREAM's somatic activity does not contribute to fertility in some form.

1 Introduction

Gene knockout experiments have proven to be useful in studying cell cycle regulation. Cell cycle regulation is established by a complex protein network and many signaling pathways that determine when a cell will or won't divide, but fundamentally the pathways center on transcriptional control of genes essential for division [1]. Moreover, the multiple cell types and tissues in multi-cellular eukaryotes each regulate the cell cycle differentially to maintain homeostasis. No two cell types are as distinct as those that make up an organism's body, called somatic cells, and those that make up an organism's reproductive system, called germ cells. Even though the two systems have widely different requirements for the cell cycle, little is known about how cell cycle regulation differs between somatic cells and germ cells. We are interested in evaluating how regulation of cell cycle quiescence, or exit from the cell cycle, differs between somatic cells and germ cells, by evaluating how the highly conserved transcriptional repressor complex called DREAM functions between the two tissue types [2]. To do so, we used tissue-specific gene knockout experiments in the model organism *Caenorhabditis elegans* to determine the tissue-specific activity of the DREAM complex in the soma and in the germline.

1.1 The Eukaryotic Cell Cycle

The eukaryotic cell cycle consists of four main stages that cells progress through for division: the G1 growth stage in which the cell prepares for DNA replication, S-phase in which the cell's DNA is replicated, the pre-mitotic G2 growth stage in which molecules required for mitotic division are synthesized,

and the M-phase mitotic stage that ends with cytokinesis. The result of the cell cycle is two identical cells that can undergo the cycle again to continue to multiply. An additional phase called the G0 stage, also known as the quiescent stage, is an alternative cell cycle state in which cells enter a reversible dormant state outside the cell cycle [3]. Quiescence is important because not all cells require ongoing division. For example, if cells were to multiply repeatedly without the ability to enter quiescence, there would be an abundance of cells which would ultimately form a tumor [4,5]. The quiescent stage prevents cells from multiplying when new cells are not needed [3].

The outcome of the cell cycle differs between somatic cells, or cells that make up an organism's body, and germ cells, or cells that make up an organism's gamete producing reproductive system. Somatic cells undergo mitosis for division resulting in two identical cells. Germ cells undergo both mitosis and meiosis to produce four non-identical haploid gametes. Meiosis involves two stages known as meiosis I and meiosis II. The end result of meiosis I is two daughter cells, similar to the result of mitotic division. In meiosis II, the daughter cells do not multiply their DNA before dividing once more, resulting in a total of four haploid cells. Understanding the differences between mitosis and meiosis in somatic cells and germ cells, respectively, highlights the ability of cell cycle dependent genes to be expressed in a tissue-specific manner [6].

The cell cycle is a highly regulated process, and disruption of cell cycle regulation leads to the over-proliferation of cells. Understanding the complex regulation of the cell cycle and cell division is important due to the fact that

deregulation may lead to a variety of diseases. Over-proliferation of somatic cells leads to tumorigenesis and can result in aggressive and metastatic cancers. On the other hand, under-proliferation of somatic cells may lead to inadequate wound healing [7]. In germ cells, disruption of cell cycle regulation leads to fertility issues [8]. Therefore, establishing a deeper understanding of cell cycle regulation and how it differs between somatic and germ cells may lead to more effective treatments for people affected by conditions such as cancers, inadequate wound healing, and infertility.

1.1.1 DREAM Complex

The DREAM complex (**D**imerization partner, **R**B-like protein, **E**2F, and **M**ulti-vulval class B) (**Figure 1**) is a highly conserved 8-subunit transcriptional repressor complex responsible for establishing the quiescent stage of the cell cycle [9]. The DREAM subcomplex Multi-vulval class B (MuvB) (**Figure 2**) is composed of five proteins (LIN-54, LIN-37, LIN-52, LIN-9, and RBBP4) [9]. MuvB is bound to DNA through the LIN-54 subunit at the cell cycle genes homology region (CHR) [10]. MuvB is unique in its ability to act as both a transcriptional activator and repressor in mammalian cells. In mammalian cells, the DREAM complex represses cell cycle genes in the G0 and G1 stages when the Rb-like pocket proteins called p107 or p130 and the MuvB subcomplex associate with a E2F-DP transcription factor heterodimer [11]. The repression of cell-cycle dependent genes causes cells to enter and maintain quiescence until the required genes are activated once more.

MuvB also acts as a transcriptional activator in stages S, G2, and M after the DREAM complex is inactivated as cells enter the cell cycle [12]. Once dissociated from the DREAM complex, MuvB associates with BMYB to form the MMB complex in mammalian organisms [12]. MMB is responsible for activating gene transcription in the S phase of the cell cycle [12]. While MMB is necessary for continuation through the cell cycle, overactivation of the MMB complex is linked to cellular over-proliferation and cancer [12].

Caenorhabditis elegans is a model organism often chosen for studying the DREAM complex and regulatory roles of the MuvB subcomplex. The DREAM complex is less complex in *C. elegans* than in mammals, making *C. elegans* an ideal candidate for studying basic DREAM function [13,14]. *C. elegans* has a clear body, allowing for visualization of the clearly differentiated germline and soma [15]. The DREAM complex is ubiquitously expressed [16]. However, previous studies focused on studying DREAM in the soma, but not the germline. Current knowledge of DREAM function in *C. elegans* does not consider potential differences in requirements for regulating the cell cycle inherent in germline cellular biology.

A primary difference between MuvB function in *C.* elegans compared to mammalian cells is that MuvB acts solely as a transcriptional repressor in *C. elegans*, and has no known activity as a transcriptional activator. This is likely due to *C. elegans* not having a homolog of BMYB, a required protein for the transcription-activating MMB complex [17]. The understanding that MuvB acts as

a transcriptional repressor in *C. elegans* enables focused studies into how the subcomplex contributes to DREAM transcriptional repression.

1.1.2 Tissue-Specific Activity of DREAM

A study on *C. elegans* performed by Kudron *et al* suggests that the DREAM complex components bind to chromatin in a tissue-specific manner. By focusing on EFL-1, DPL-1, and LIN-35 chromatin binding activity in somatic, germline, and intestinal tissues *in* vivo, Kudron *et* al revealed that the DREAM components bind to different genomic sites in somatic and germline tissues [14]. While it's believed that the DREAM complex regulates gene expression and cell fate determination, how DREAM acts differently in somatic versus germline tissues with regards to gene regulation has not yet been elucidated

Interestingly, DREAM components were first identified as Synmuv class B genes, which are a group of regulatory genes that are responsible for cell differentiation in somatic tissues, including the vulva. The Synmuv B pathway functions to prevent germline gene expression in the soma, also called soma-to-germline transformation [18]. Characteristics of germline fate include RNAi sensitivity, ectopic expression of germline genes, and increased transgene silencing [19]. In *C. elegans*, soma-to-germline transformation is known to result in a high-temperature larval arrest phenotype (HTA) [18,20]. Another study showed that mutation of *lin-35* causes reduced fertility of *C. elegans* [21].

The DREAM complex functions to repress germline gene expression in the soma [18], but not much is known regarding DREAM function in the germline. Kudron *et al* showed that germline LIN-35 was unable to rescue the HTA

phenotype in somatic *lin-35* mutants. However, germline LIN-35 was able to rescue the reduced fertility phenotype of germline *lin-35* mutants [14]. These results suggest that DREAM function may differ between somatic cells and germ cells.

1.1.3 Auxin-Inducible Degron System

Gene knockdown is an effective method for studying gene function. RNA interference (RNAi) is commonly used for observing the effects of gene knockdown *in vivo* [22,23]. However, there are drawbacks to RNAi such as unintended off-target effects [23,24]. In RNAi experiments, there may be target protein still present due to the RNAi attacking mRNA, leaving any previously translated protein to remain functional [25].

Developed in 2009, the auxin-inducible degron system (AID) is a powerful tool for the fast and reversible depletion of protein [26]. The ability of the AID system to deplete a targeted protein within a few hours allows for phenotypic observations to be made before secondary effects may manifest [26].

The components of the AID system (**Figure 3**) include the SCF E3 ubiquitin ligase and the auxin family of phytohormones [26]. The SCF complex is composed of Skp1, Cullin 1, and F-box proteins [23,27]. TIR1 is an F-box protein and auxin receptor [28]. Derived from *Arabidopsis thaliana*, transgenic *At*TIR1 contains mutations D170E and M473L, which were introduced to increase auxin affinity, allowing for more reliable protein degradation [29]. Because the other components of the SCF complex are highly conserved, driving transgenic TIR1 using different promoters enables tissue-specific targeting of the AID system. For

example, in *C. elegans*, the *eft-3* promoter drives TIR1 expression solely in somatic cells while the *rps-28* promoter drives TIR1 expression ubiquitously in both somatic and germ cells [30]. The ability to target specific cell types makes the AID system useful for studying the tissue-specific activity of the DREAM complex.

Use of the AID system in *C. elegans* requires the fusing of a 44 amino acid degron sequence to a protein of interest along with a reporter such as GFP for visualization of protein depletion under a fluorescence microscope [31]. TIR1 recognizes and binds to the degron sequence in the presence of auxin. The target protein is then marked by E3 ubiquitin ligase for proteasomal degradation [26,32].

Drawbacks to using the AID system include leaky degradation, where target protein degradation occurs in the absence of auxin [33,34,35,36] and the need for high doses of auxin which can increase the lifespan of *C. elegans* [37], changing a fundamental characteristic of the organism. These drawbacks make it more difficult to observe the effects of gene knockout *in vivo*.

The drawbacks of the AID system have been addressed with the development of the auxin-inducible degron 2 (AID2) system [36,38]. The AID2 system differs from the AID system in that *At*TIR1 is mutated to contain the F79G mutation observed in *Os*TIR1, a TIR1 protein derived from *Oryza sativa* [36,38]. Negishi *et al* tested AID2 in *C. elegans* by inserting an *At*TIR1(F79G) transgene into the genome, and observed the occurrence of leaky degradation in the

original AID system was mitigated in the AID2 system. The study found that the AID2 system provided a remedy for the drawbacks of using the AID system [36].

1.1.4 Study Hypothesis

The purpose of this project is to observe the consequences of gene knockdown in the *C. elegans* DREAM complex on germline function. As previously mentioned, a study investigating the tissue-specificity of DREAM has shown that there are different binding profiles of DREAM among various tissue types [14]. While this study observed a lack of LIN-35 binding in the *C. elegans* germline, the researchers did not investigate MuvB function in the *C. elegans* germline.

This project aims to expand upon the current knowledge of DREAM activity in the germline by knocking down LIN-54 or LIN-35 in the *C. elegans* germline. To accomplish this, the auxin-inducible degron 2 (AID2) system was used to rapidly deplete the protein of interest in both somatic and germ cells. The consequences of gene knockdown were observed in *C. elegans* exposed to auxin, as compared to vehicle control. It was expected that the F1 generation of *C. elegans* exposed to auxin in the ubiquitously-expressed TIR1 strain would be sterile due to lacking LIN-54 in the germline [39], or have reduced fertility due to LIN-35 germline degradation [21]. However, we observed loss of fertility in both TIR1-expressing strains. Using fluorescence microscopy, we observed that the somatically-expressed TIR1 strain experienced degradation of LIN-54 or LIN-35 in the germline. The current AID2 system in our *C. elegans* model does not appear to be successful in achieving complete tissue-specificity for protein

depletion. However, the partial protein depletion that was qualitatively observed in the germline has still provided insight into MuvB function in the *C. elegans* germline.

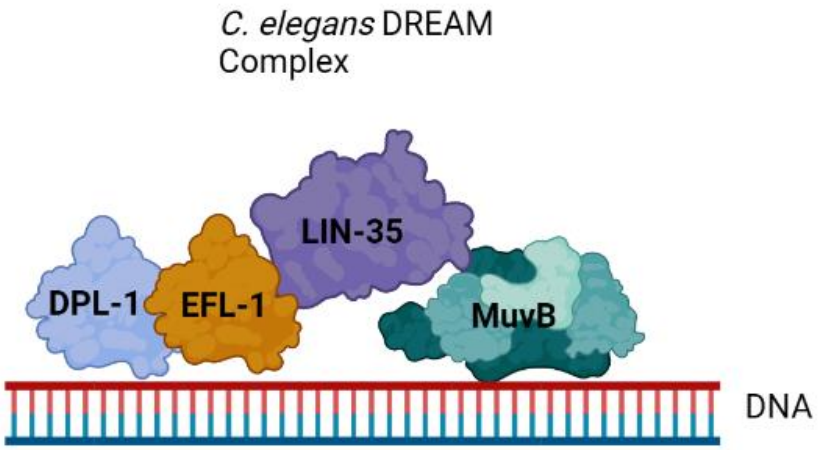

Figure 1 DREAM complex in *C. elegans*

The **D**imerization partner, **E**2F, **R**b-like, **a**nd **M**uvB complex is responsible for repression of cell cycle-dependent genes. Created with BioRender.com

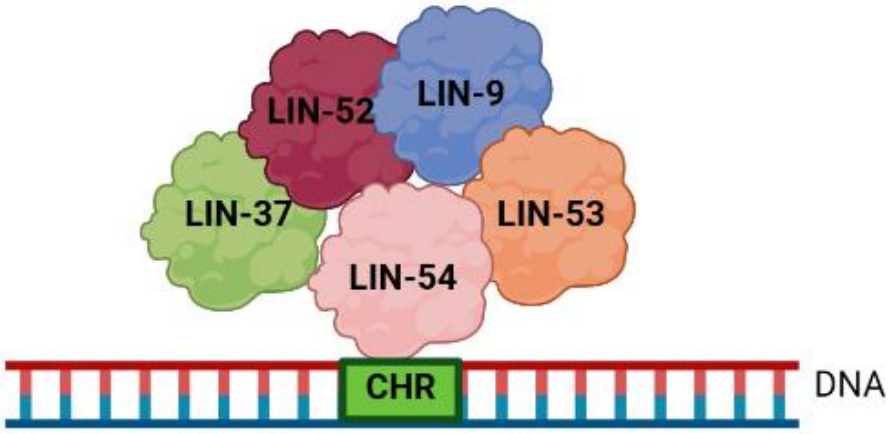

Figure 2 MuvB Subcomplex in *C. elegans*

The MuvB subcomplex in *C. elegans* is composed of five subunits: LIN-54, LIN-37, LIN-52, LIN-9, and LIN-53. Created with BioRender.com

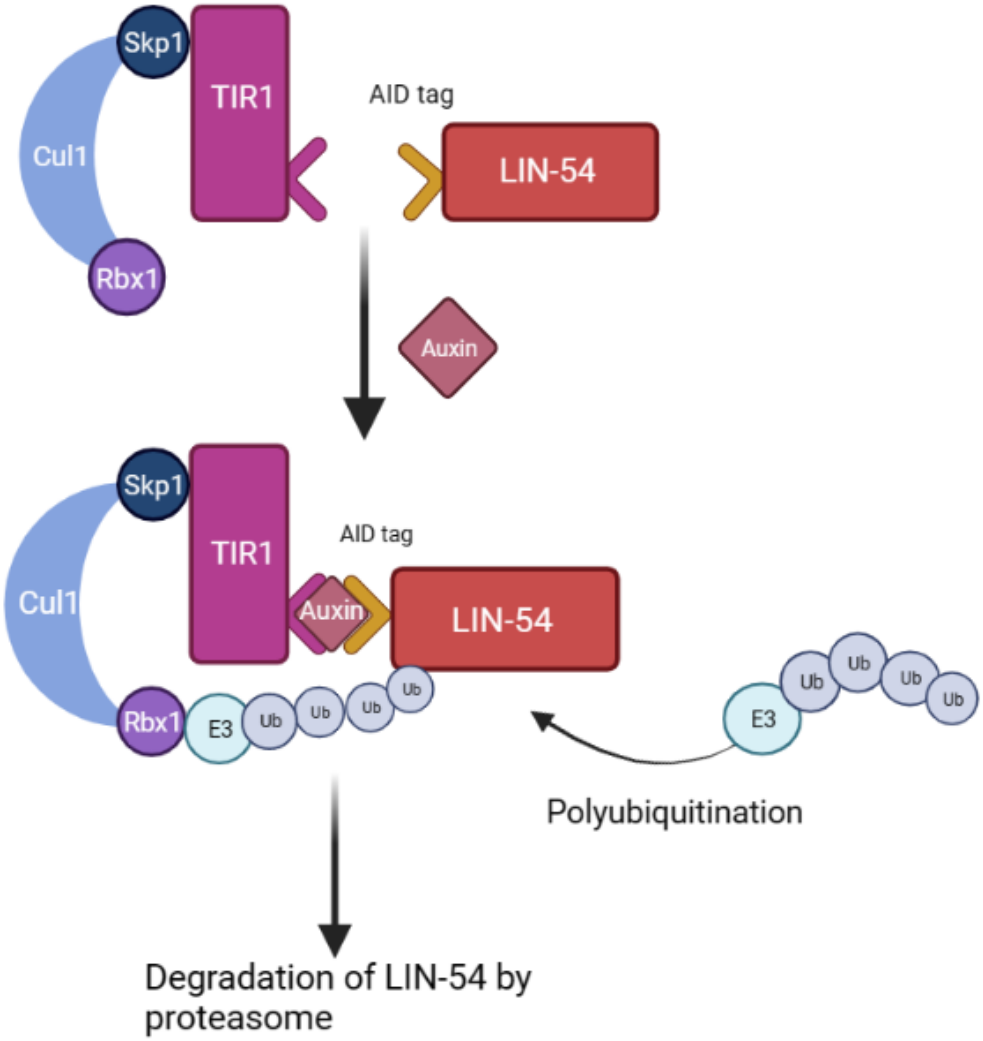

Figure 3 The Auxin-Inducible Degron System

The auxin-inducible degron (AID) system requires an SCF complex, auxin, and a tagged protein of interest. The SCF complex is made up of Cul1, Rbx1, Skp1, and TIR1. When auxin is introduced, Skp1 binds to TIR1 and the tagged protein of interest. Upon binding of auxin, an E3-Ubiquitin complex is recruited to Rbx1 resulting in polyubiquitination of the protein of interest. Proteasomal degradation of the protein of interest follows.

1.2 Materials and Methods

1.2.1 Worm Strains

LIN-54 tagged strains:

1. cshIs140 [*rps-28p::TIR1(F79G)::T2A::mCherry::his-11* + *Cbr-unc-119(+)*] II; *lin-54::GFP-AID-3xFLAG* IV
2. osIs158 [*eft-3p::ccvTIR-1(F79G)::mRuby*] II; *lin-54::GFP-AID-3xFLAG* IV

LIN-35 tagged strains:

1. cshIs140 [*rps-28p::TIR1(F79G)::T2A::mCherry::his-11* + *Cbr-unc-119(+)*] II; *lin-35(kea7[lin-35p::degron::GFP::lin-35])* I
2. osIs158 [*eft-3p::ccvTIR-1(F79G)::mRuby*] II; *lin-35(kea7[lin-35p::degron::GFP::lin-35])* I

1.2.2 Worm Maintenance

Worms were fed *Escherichia coli* strain, OP50, on agar plates. Every four days, three worms at the L4 or young adult stage were transferred to a new agar plate containing OP50, and then incubated at 20℃.

1.2.3 Brood Counting Experiments

To establish the parent (P0) generation, three worms at the L4 stage were transferred to either a vehicle (control) agar plate containing OP50, or an experimental plate containing OP50 and 1μM 5-phenyl-indole-3-acetic acid (5-Ph-IAA, referred to as auxin). After approximately two days, the parent generation produced progeny. The newly hatched worms were designated as the F1 generation. One worm from the F1 generation that was hatched on the auxin

P0 plate was then moved to a new auxin plate. One worm from the F1 generation that was hatched on the vehicle P0 plate was then moved to a new vehicle plate. All F1 worms were transferred to the new plates at the L4 larval stage. This process was repeated a total of 8 times. For strains that experienced a high frequency of premature worm death, the number of worm plates were increased to validate the results.

Each day following the worm transfer, the progeny observed on each plate were counted. The progeny of the F1 generation were designated as the F2 generation. Each F2 generation worm was flamed after being counted to avoid counting the same worm twice. This process was repeated until the F1 generation worm stopped laying embryos, and the laid embryos finished hatching. The worm counts for each counting session were recorded at the end of each session, and were totaled at the conclusion of the final session. In the instance of the F1 generation worm unexpectedly dying, any progeny from the F1 generation worm was counted, and the death of the F1 generation worm was recorded.

1.2.4 Dissection of *C. elegans*

The day before dissection, the worms were prepared by transferring 20 old L3/young L4 worms of each strain to vehicle (control) and auxin (treatment) plates, respectively. These plates were incubated overnight at 20℃.

To perform the dissection, 20mM of levamisole was placed onto a glass slide. For each worm strain, 3 worms at the L4/young adult stages were picked off the plate and placed into the levamisole. Once worm movement ceased, a

needle attached to a syringe was used to slice the posterior end of the worm open. Due to the internal pressure in the worm, the germline was pushed out of the worm upon the removal of the posterior end. As soon as the posterior end of each worm had been removed, a coverslip with 3µL of S basal buffer was placed on top of the glass slide to keep the dissected worms in place. Immediately following dissection, the worms were imaged to avoid swelling occurring as time passed since worm death. Further dissections were performed following the imaging of the previous set of 3 worms. This process was repeated for both the auxin-treated and vehicle worms from each strain.

1.2.5 Fluorescent Imaging of the *C. elegans* germline

Fluorescent imaging was performed using a Zeiss Axioskop 2 with a SOLA FISH LED Light Engine and Panda 4.2 Monochrome sCMOS Camera. Images were acquired using µManager software [40]. The exposure was set to 500 ms to allow for more visibility when using the 40x objective to view the germline. Images were taken with the brightfield light on without the fluorescence to show the normal view of the germline, followed by images with the LED excitation on without the brightfield light to visualize the fluorescence.

1.3 Results

1.3.1 LIN-54 degradation in all cell types causes decreased brood size

We first evaluated the effects following degradation of LIN-54, a subunit of the DREAM's MuvB subcomplex. Ubiquitous expression of TIR1 in the *rps-28*p-

TIR1 transgenic strain with degron-tagged LIN-54 showed a decreased brood size in the auxin-treated experimental group. This strain, when exposed to auxin, was expected to induce degradation of LIN-54 in both the soma and the germline. On average, the brood size of the auxin-exposed experimental group was 138 progeny. On average, the brood size of the control group was 302 progeny (**Table 1**,**Figure 4**). Table 1 depicts the raw data collected from the brood counting experiments. Data designated with an asterisk signifies premature worm death, and we excluded these progeny counts from our statistical analysis. Because the worm's death was not replicated, we did not further investigate the potential cause.

The null hypothesis states there was no significant difference between the progeny counts of auxin-treated and vehicle *C. elegans* of this strain. The alternative hypothesis states there was a significant difference between the progeny counts of auxin-exposed and non-exposed *C. elegans* of this strain. A two-tailed unpaired T-test resulted in a p-value of 3.2×10^{-5}. At a 99% confidence interval ($p<0.01$), this p-value is low enough to reject the null hypothesis in favor of the alternative. Our results suggest that LIN-54 protein in the soma and/or the germline is important to maintain *C. elegans* fertility.

Fluorescent imaging of the germline revealed that LIN-54 is not completely knocked out in the germline. Germlines from the auxin *rps-28*p-TIR1 transgenic strain with degron-tagged LIN-54 showed fluorescence indicating the presence of LIN-54 despite auxin treatment (**Figure 5**,**Figure 6**,**Figure 7**). The fluorescence of the treated worms visually appears to be less intense than that of the non-

treated worms (**Figure 5**,**Figure 6**,**Figure 7**). The difference in fluorescence intensity suggests that although there is LIN-54 expression in the germline of the treated worms, there is less expression than normal.

1.3.2 High lethality after auxin exposure in *eft-3*p-TIR1 transgenic strain with degron-tagged LIN-54

We next evaluated LIN-54 degradation in the *eft-3*p-TIR1 transgenic strain with degron-tagged LIN-54 which drives TIR-1 expression in somatic cells only. This strain showed an unexpectedly high number of premature worm deaths in the auxin-exposed experimental group. To verify that the worm deaths were not independent of experimental condition, the number of plates observed were increased from the base 8 to 13 auxin-treated plates, and 12 vehicle plates as the control. In the auxin-exposed experimental group, 10 out of 13 worms exposed to auxin prematurely died before a complete brood could be laid, rendering the data from these worms unusable. Of the 10 deceased worms, 5 experienced bagging. Bagging is a phenomenon in which the *C. elegans* die before laying embryos, allowing the embryos to hatch inside the deceased worm. Of the three auxin-treated worms that survived to adulthood, the brood sizes were 58, 191, and 209, respectively (**Table 2**). On average, the brood size of the control group was 283 progeny (**Table 2**,**Figure 8**).

Fluorescent imaging of the *eft-3*p-TIR1 transgenic strain with degron-tagged LIN-54 showed diverse effects of auxin treatment on the germline. Due to the *eft-3* promoter only expected to drive TIR1 expression in somatic cells, it was unexpected to observe LIN-54 degradation in the germline. Observing a lack of

fluorescence in the germlines of these worms suggests that germ cells are also being affected by the AID2 system in this strain and also indicates that the *eft-3p* expressed TIR1 at some level in the germline (**Figure 10**). Figure 10 depicts a germline showing lower fluorescence in the germ cells suggesting partial LIN-54 depletion, but high fluorescence in the oocytes. This is consistent with previous findings suggesting that some forms of auxin are not able to permeate the eggshell [36]. The bagging phenomenon may also be explained by the inability of auxin to permeate the eggshell. It is possible that the F1 worm was no longer able to survive due to LIN-54 depletion, but its embryos remained unaffected, leading to hatching within the deceased worm.

The germline depicted in Figure 9 shows higher fluorescence than Figures 10 and 11 despite all images being taken under the same conditions (**Figure 9**,**Figure 10**,**Figure 11**). This result suggests that the amount of LIN-54 degradation in the germline may vary in the *eft-3*p-TIR1 transgenic strain with degron-tagged LIN-54.

1.3.3 LIN-35 Degradation in all cell types causes decreased brood size

Brood counting experiments of the *rps-28*p-TIR1 transgenic strain with degron-tagged LIN-35 resulted in an average brood size of 335 and 284 worms for auxin-treated and vehicle groups, respectively, rounded up to the nearest whole number (**Table 3**). Statistical analysis revealed there was no statistically significant difference in brood size in auxin-treated and vehicle groups (p=0.013,

p<0.01) in the *rps-28*p-TIR1 transgenic strain with degron-tagged LIN-35 (**Figure 12**).

Brood counting experiments of the *eft-3*p-TIR1 transgenic strain with degron-tagged LIN-35 resulted in an average brood size of 254 and 320 for auxin-treated and vehicle groups, respectively, rounded up to the nearest whole number (**Table 4**). Statistical analysis revealed there was a statistically significant difference in brood size in auxin-treated and vehicle groups in the *eft-3*p-TIR1 transgenic strain with degron-tagged LIN-35 (p=0.002, p<0.01) (**Figure 16**).

Fluorescent imaging showed that there was some decreased expression of LIN-35 in the auxin-treated *rps-28*p-TIR1 transgenic strain with degron-tagged LIN-35 (**Figure 13**,**Figure 14**,**Figure 15**) compared to the vehicle group (**Figure 13**,**Figure 14**,**Figure 15**). Of the germlines imaged for the auxin-treated *rps-28*p-TIR1 transgenic strain with degron-tagged LIN-35, Figure 13 shows the least intense fluorescence, observed qualitatively (**Figure 13**). Interestingly, fluorescent imaging showed that there was degradation of LIN-35 in the auxin-treated *eft-3*p-TIR1 transgenic strain with degron-tagged LIN-35 (**Figure 17**,**Figure 18**,**Figure 19**) compared to the vehicle group (**Figure 17**,**Figure 18**,**Figure 19**). The vehicle groups showed approximately the same level of expression, observed qualitatively.

Fluorescence microscopy revealed that LIN-35 was degraded more extensively in the germline of the auxin-treated *eft-3p*-TIR1 transgenic strain with degron-tagged LIN-35 (**Figure 17**,**Figure 18**,**Figure 19**) compared to the auxin-treated *rps-28*p-TIR1 transgenic strain with degron-tagged LIN-35 (**Figure**

13,**Figure 14**,**Figure 15**), suggesting that germline degradation causes decreased brood size.

Plate #	Auxin-Treated	Vehicle
1	172	261
2	193	235
3	211	314
4	66	339
5	137	300
6	40	325
7	137	14*
8	146	339
Average	137.75	301.86
Standard Deviation	58.99	39.99

Table 1 Brood sizes of *rps-28*p-TIR1 transgenic strain with degron-tagged LIN-54

Table showing the brood sizes of *rps-28*p-TIR1 transgenic strain with degron-tagged LIN-54.

*=Data excluded from the average, standard deviation, and statistical testing due to worm death.

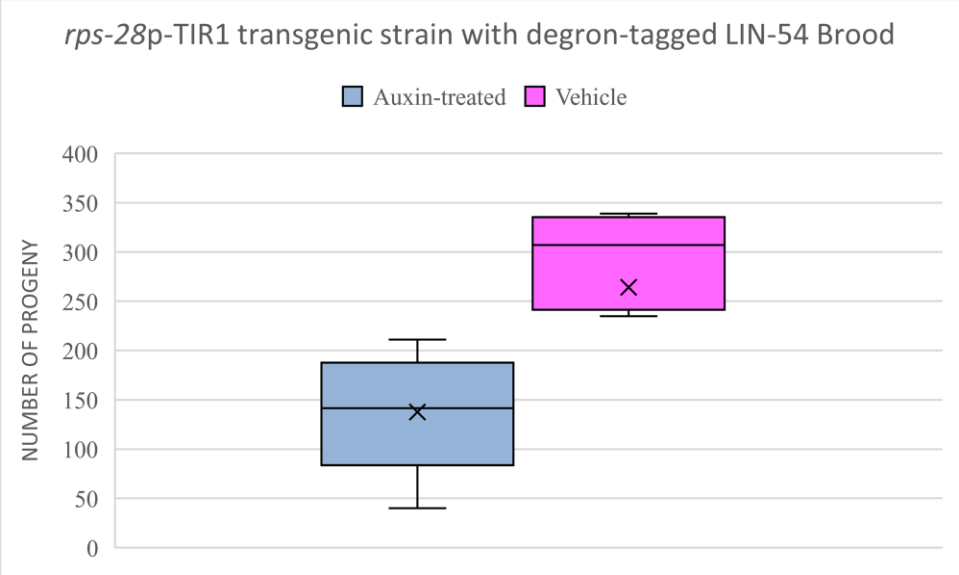

Figure 4 *rps-28*p-TIR1 transgenic strain with degron-tagged LIN-54 brood counting experiment

Box-and-whisker chart comparing the effect of auxin treatment vs vehicle on brood size in the *rps-28*p-TIR1 transgenic strain with degron-tagged LIN-54. The average is designated by "X". Significance testing was performed with a two-tailed unpaired T-test. The p-value associated with this data is 3.2×10^{-5}. A 99% confidence interval was used with $p<0.01$ as the requirement to reject the null hypothesis.

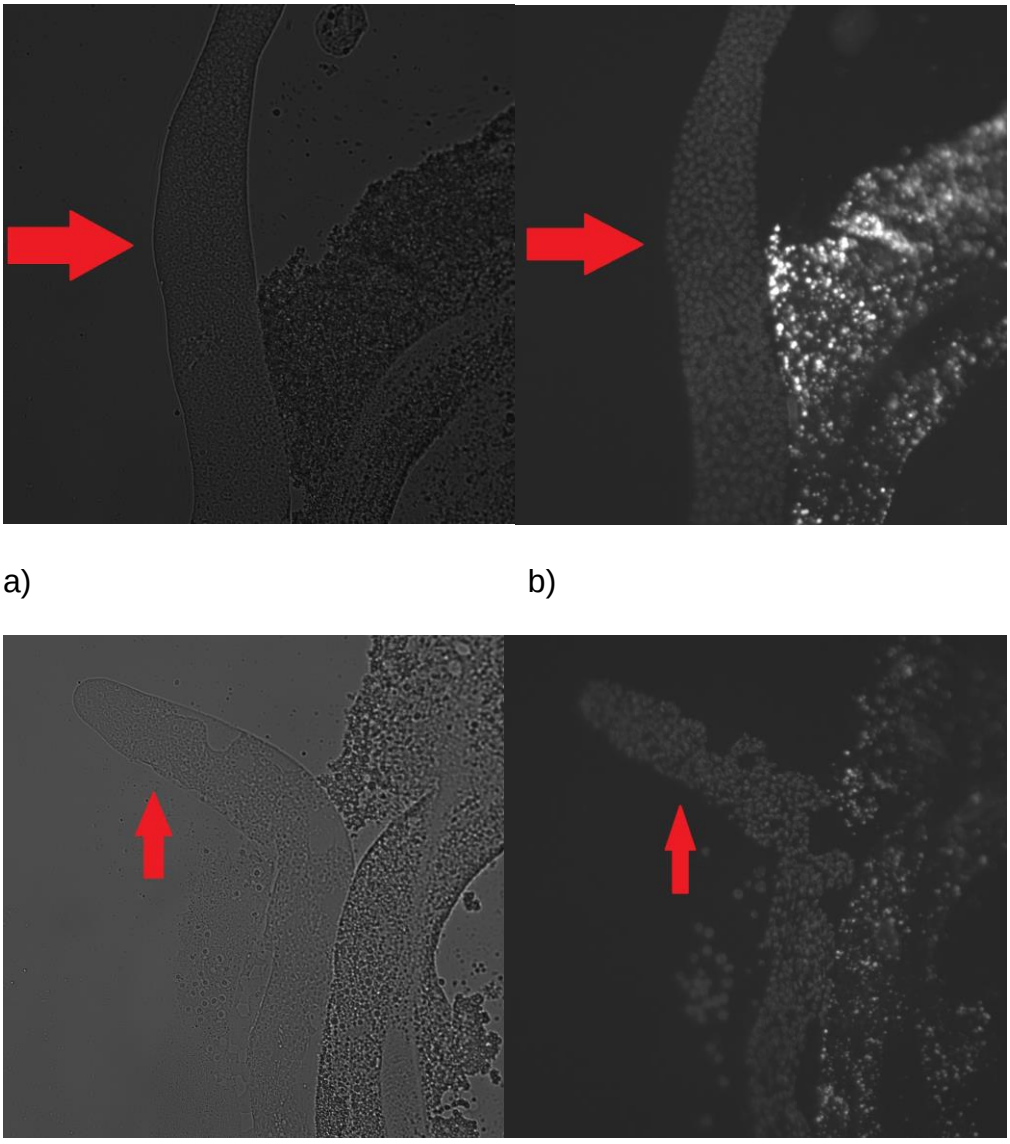

Figure 5 *rps-28*p-TIR1 transgenic strain with degron-tagged LIN-54 Fluorescent Imaging 1

Images of auxin-treated *rps-28*p-TIR1 transgenic strain with degron-tagged LIN-54 under normal light (a) and fluorescence (b). Images of vehicle *rps-28p*-TIR1 transgenic strain with degron-tagged LIN-54 under normal light (c) and fluorescence (d). Germline is indicated by an arrow.

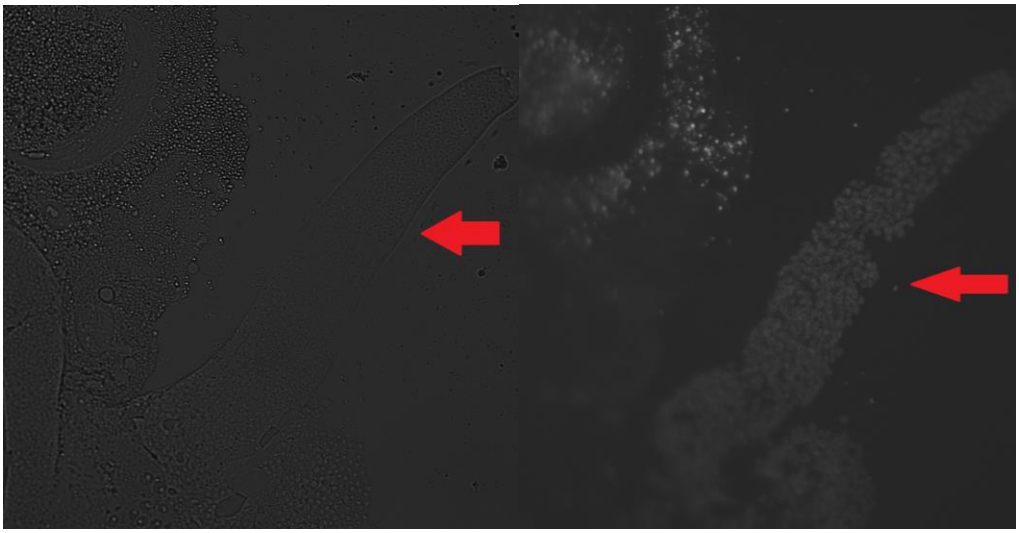

a) b)

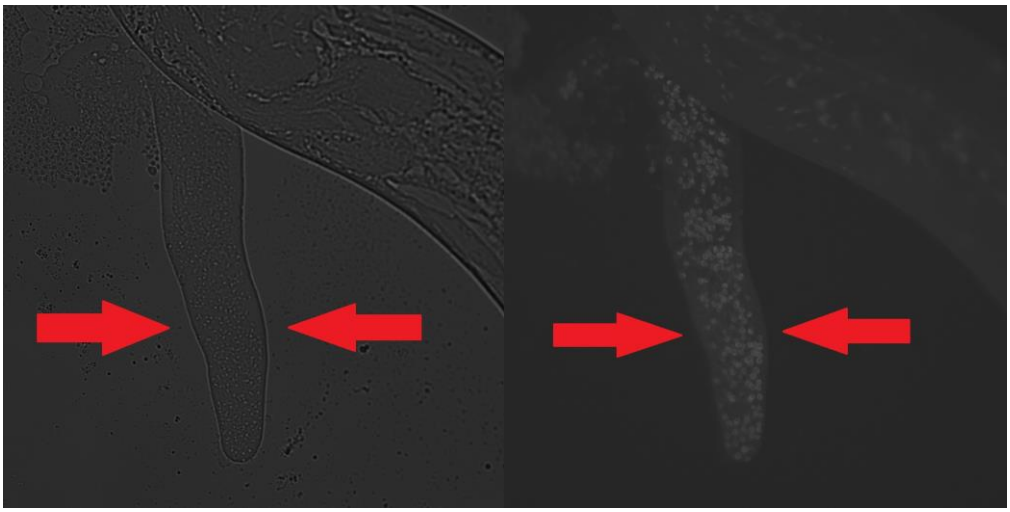

c) d)

Figure 6 *rps-28*p-TIR1 transgenic strain with degron-tagged LIN-54 Fluorescent Imaging 2

Images of auxin-treated *rps-28*p-TIR1 transgenic strain with degron-tagged LIN-54 under normal light (a) and fluorescence (b). Images of vehicle *rps-28p*-TIR1 transgenic strain with degron-tagged LIN-54 under normal light (c) and fluorescence (d). Germline is indicated by an arrow.

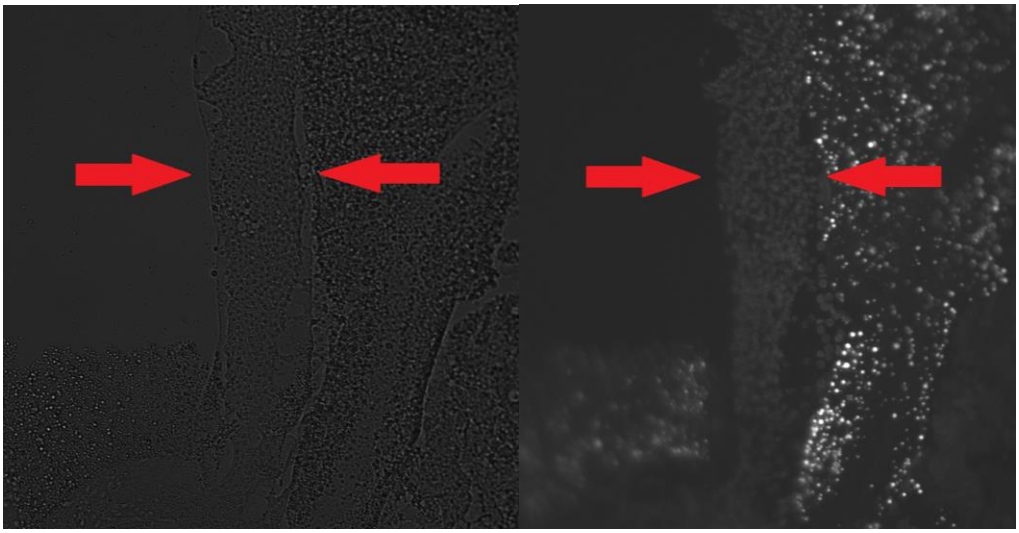

a) b)

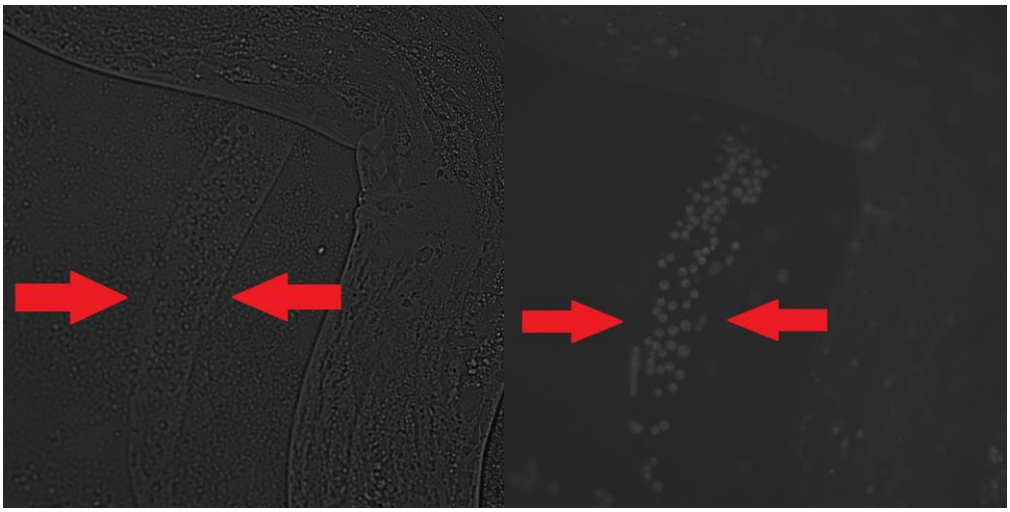

c) d)

Figure 7 *rps-28*p-TIR1 transgenic strain with degron-tagged LIN-54 Fluorescent Imaging 3

Images of auxin-treated *rps-28*p-TIR1 transgenic strain with degron-tagged LIN-54 under normal light (a) and fluorescence (b). Images of vehicle *rps-28p*-TIR1 transgenic strain with degron-tagged LIN-54 under normal light (c) and fluorescence (d). Germline is indicated by an arrow.

Plate #	Auxin-treated	Vehicle
1	58	301
2	32*	318
3	191	320
4	29*	277
5	35**	238
6	1**	264
7	20**	312
8	209	246
9	104*	204
10	27*	286
11	0**	304
12	95**	316
13	0*	
Average	152.67	282.17
Standard Deviation	82.48	37.32

Table 2 Brood sizes of *eft-3*p-TIR1 transgenic strain with degron-tagged LIN-54

Table depicting progeny counts of the *eft-3*p-TIR1 transgenic strain with degron-tagged LIN-54. Data from the auxin-treated group that represents a complete brood is highlighted. The remaining data in the auxin-treated group is unusable, but is provided to show progeny the prematurely deceased worm.

*=Data excluded from the average, standard deviation, and statistical testing due to a worm death.

**=Bagging observed in deceased worms.

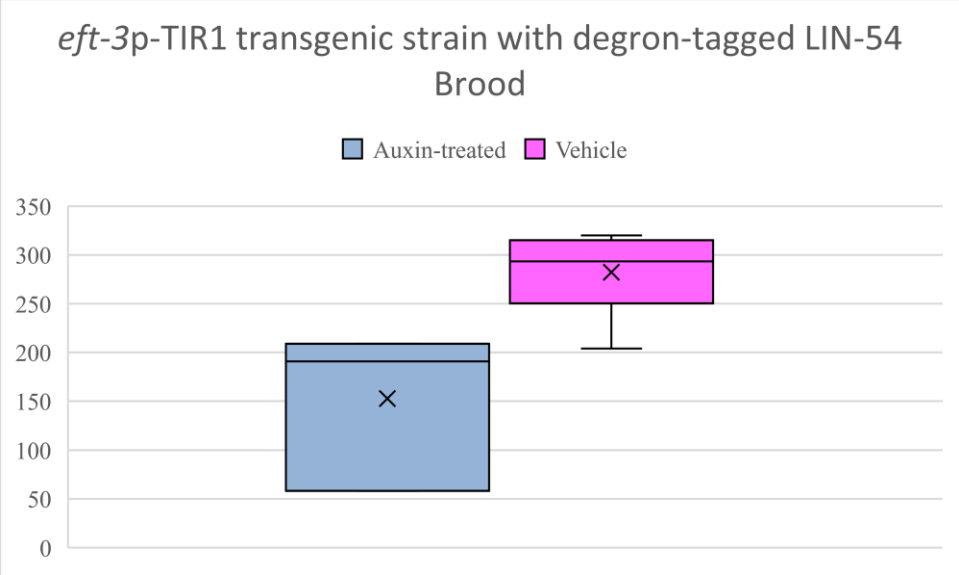

Figure 8 *eft-3*p-TIR1 transgenic strain with degron-tagged LIN-54 brood counting experiment

Box-and-whisker chart comparing the effect of auxin treatment vs vehicle on brood size in the *eft-3*p-TIR1 transgenic strain with degron-tagged LIN-54. The average is designated by “X”. Accurate statistical testing cannot be conducted due to high lethality in the auxin-treated group. Statistical testing will show a significant difference in brood size, but will not consider the inability of deceased worms to have a complete brood.

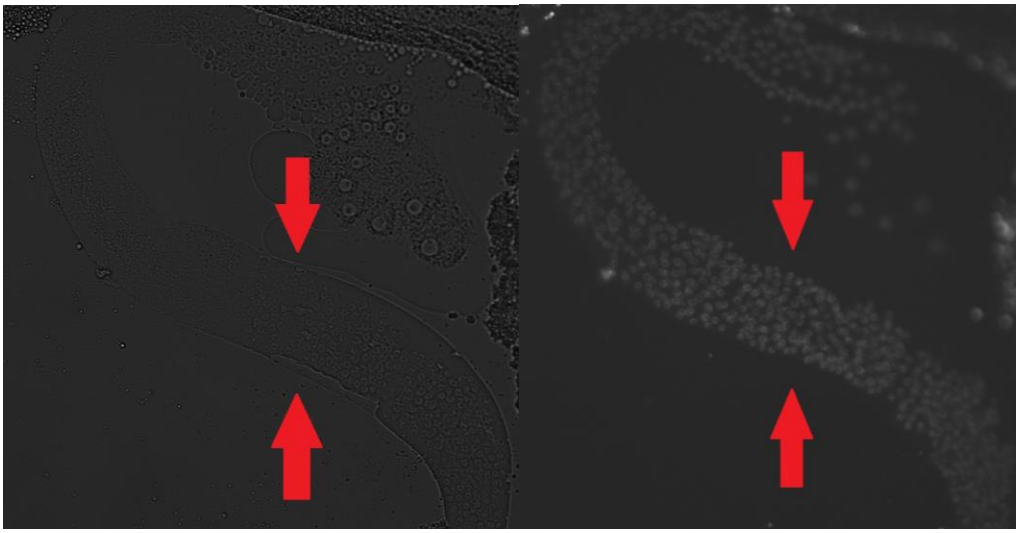

a) b)

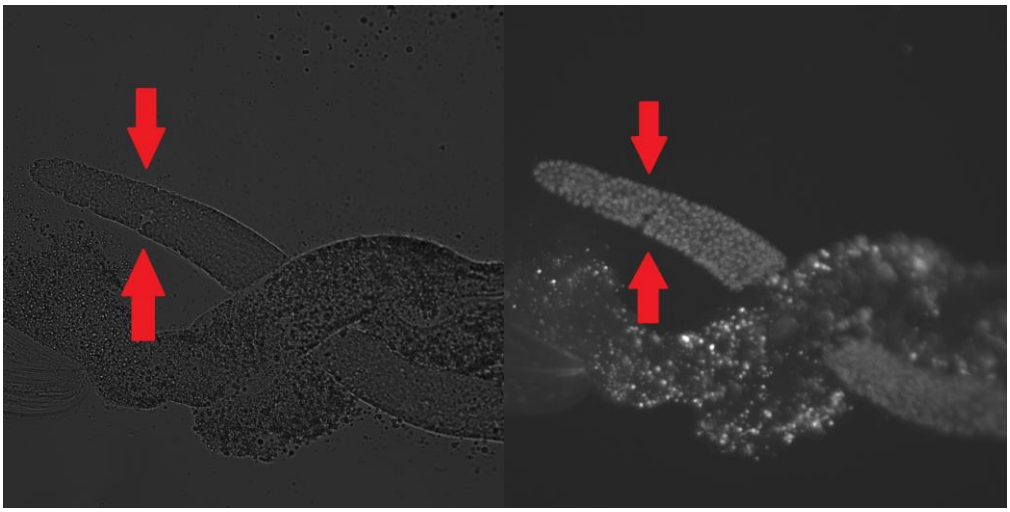

c) d)

Figure 9 *eft-3*p-TIR1 transgenic strain with degron-tagged LIN-54 Fluorescent Imaging 1

Images of auxin-treated *eft-3*p-TIR1 transgenic strain with degron-tagged LIN-54 under normal light (a) and fluorescence (b). Images of vehicle *eft-3*p-TIR1 transgenic strain with degron-tagged LIN-54 under normal light (c) and under fluorescence (d). Germline is indicated by an arrow.

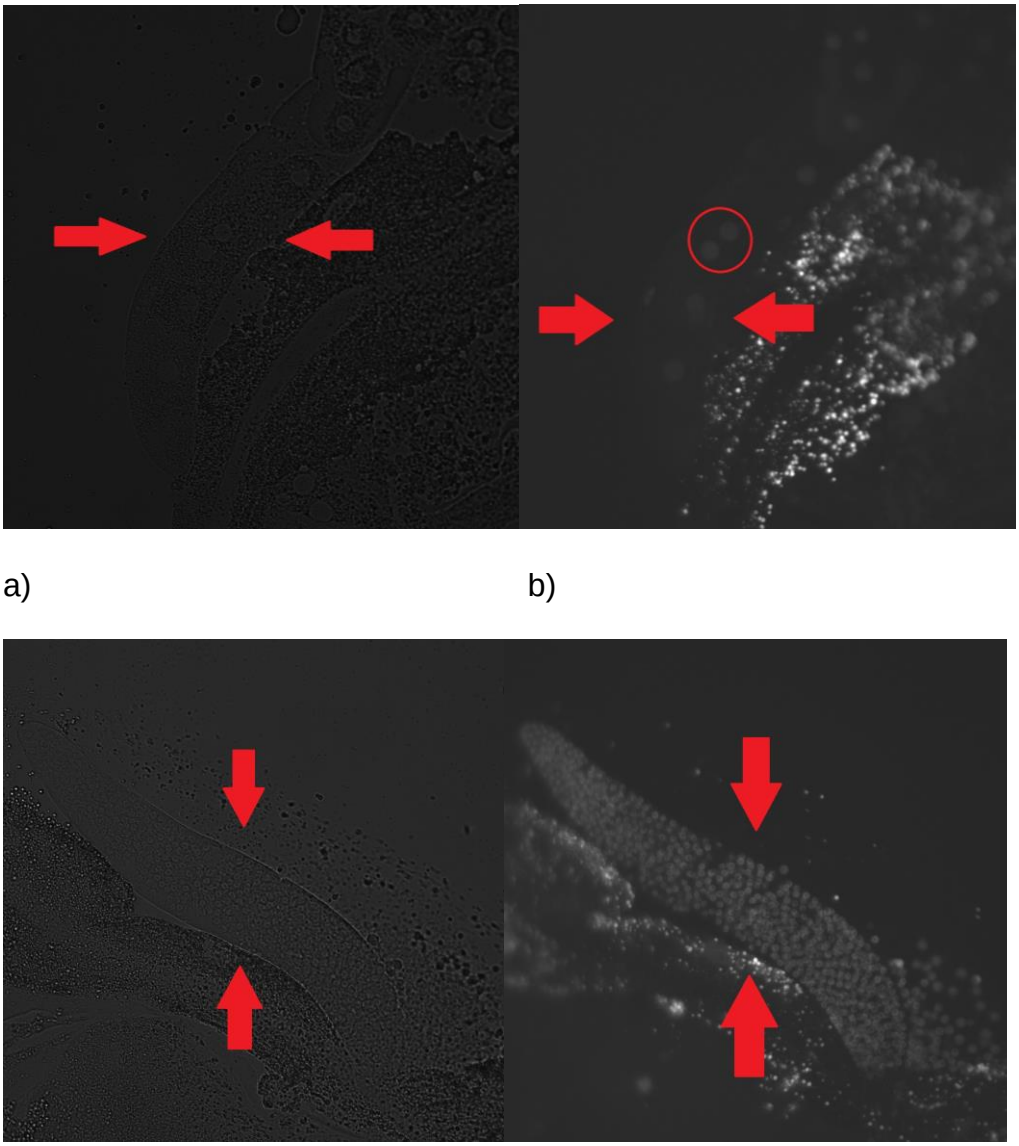

a) b)

c) d)

Figure 10 *eft-3*p-TIR1 transgenic strain with degron-tagged LIN-54 Fluorescent Imaging 2

Images of auxin-treated *eft-3*p-TIR1 transgenic strain with degron-tagged LIN-54 under normal light (a) and fluorescence (b). Images of vehicle *eft-3*p-TIR1 transgenic strain with degron-tagged LIN-54 under normal light (c) and under fluorescence (d). Germline is indicated by an arrow. Oocyte indicated by a circle.

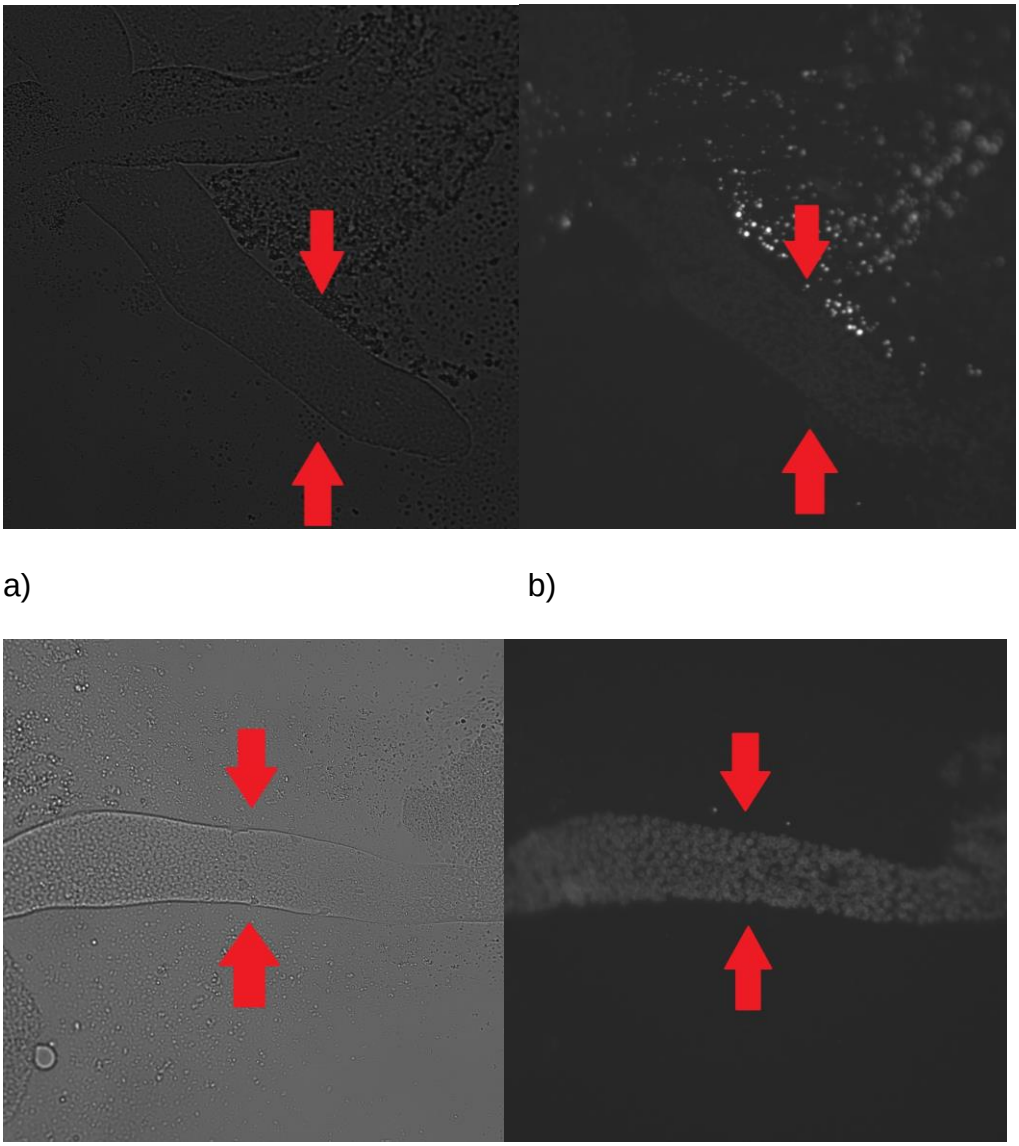

a) b)

c) d)

Figure 11 *eft-3*p-TIR1 transgenic strain with degron-tagged LIN-54 Fluorescent Imaging 3

Images of auxin-treated *eft-3*p-TIR1 transgenic strain with degron-tagged LIN-54 under normal light (a) and fluorescence (b). Images of vehicle *eft-3*p-TIR1 transgenic strain with degron-tagged LIN-54 under normal light (c) and under fluorescence (d). Germline is indicated by an arrow.

Plate #	Auxin-treated	Vehicle
1	260	257
2	5*	251
3	173	292
4	283	334
5	231	314
6	211	234
7	247	303
8	237	322
Average	234.57	288.38
Standard Deviation	35.38	36.71

Table 3 Brood sizes of *rps-28*p-TIR1 transgenic strain with degron-tagged LIN-35

Table depicting progeny counts of the *rps-28*p-TIR1 transgenic strain with degron-tagged LIN-35.

*=Data excluded from the average, standard deviation, and statistical testing due to worm death independent of experimental condition.

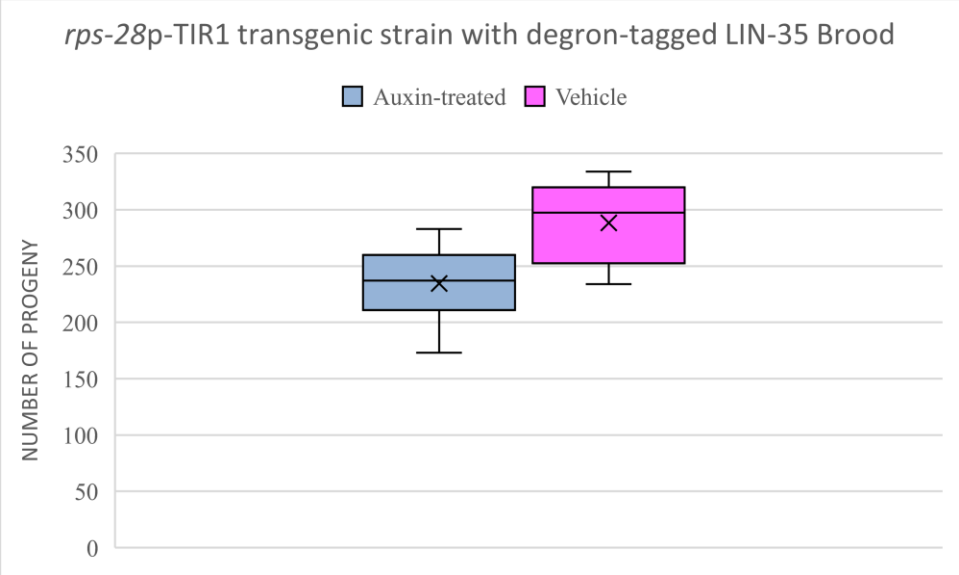

Figure 12 *rps-28*p-TIR1 transgenic strain with degron-tagged LIN-35 brood counting experiment

Box-and-whisker chart comparing the effect of auxin treatment vs vehicle on brood size in the *rps-28*p-TIR1 transgenic strain with degron-tagged LIN-35. The average is designated by “X”. Significance testing was performed with a two-tailed unpaired T-test. The p-value associated with this data 0.013. A 99% confidence interval was used with $p<0.01$ as the requirement to reject the null hypothesis.

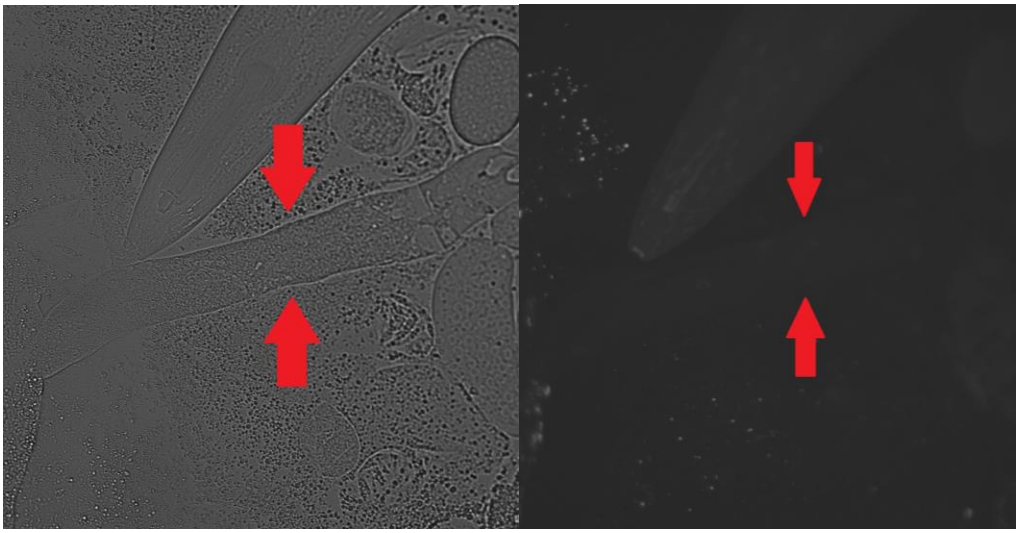

a) b)

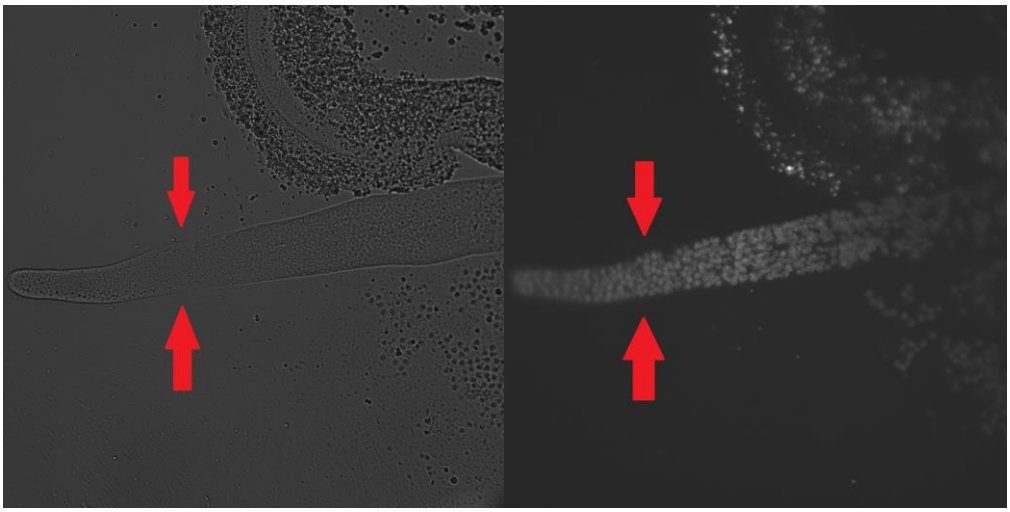

c) d)

Figure 13 *rps-28*p-TIR1 transgenic strain with degron-tagged LIN-35 Fluorescent Imaging 1

Images of auxin-treated *rps-28*p-TIR1 transgenic strain with degron-tagged LIN-35 under normal light (a) and fluorescence (b). Images of vehicle *rps*-28p-TIR1 transgenic strain with degron-tagged LIN-35 under normal light (c) ad fluorescence (d). Germline is indicated by an arrow.

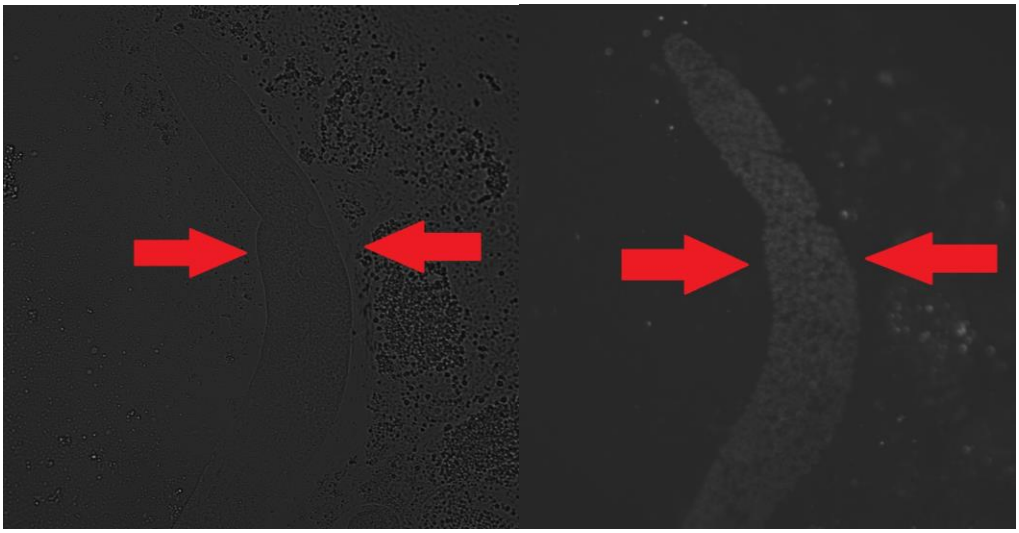

a) b)

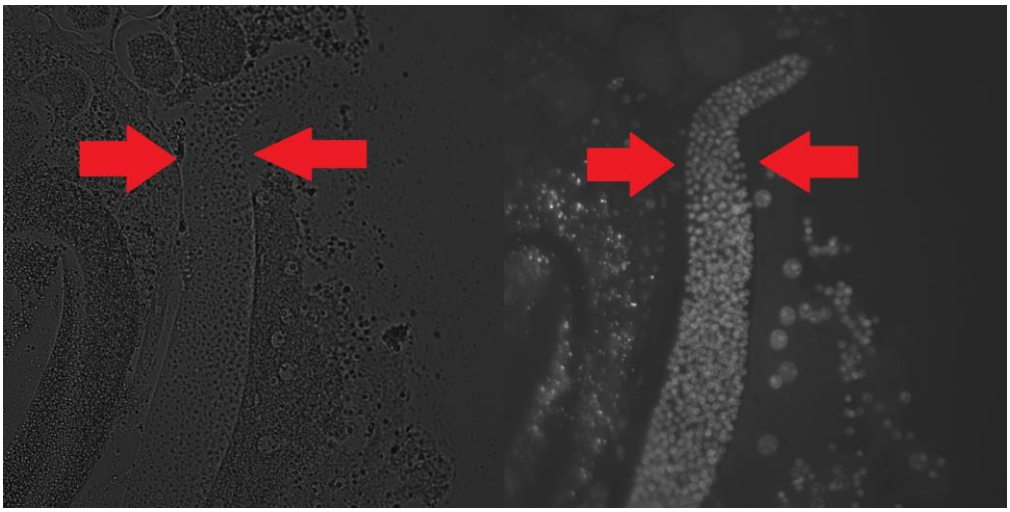

c) d)

Figure 14 *rps-28*p-TIR1 transgenic strain with degron-tagged LIN-35 Fluorescent Imaging 2

Images of auxin-treated *rps-28*p-TIR1 transgenic strain with degron-tagged LIN-35 under normal light (a) and fluorescence (b). Images of vehicle *rps*-28p-TIR1 transgenic strain with degron-tagged LIN-35 under normal light (c) ad fluorescence (d). Germline is indicated by an arrow.

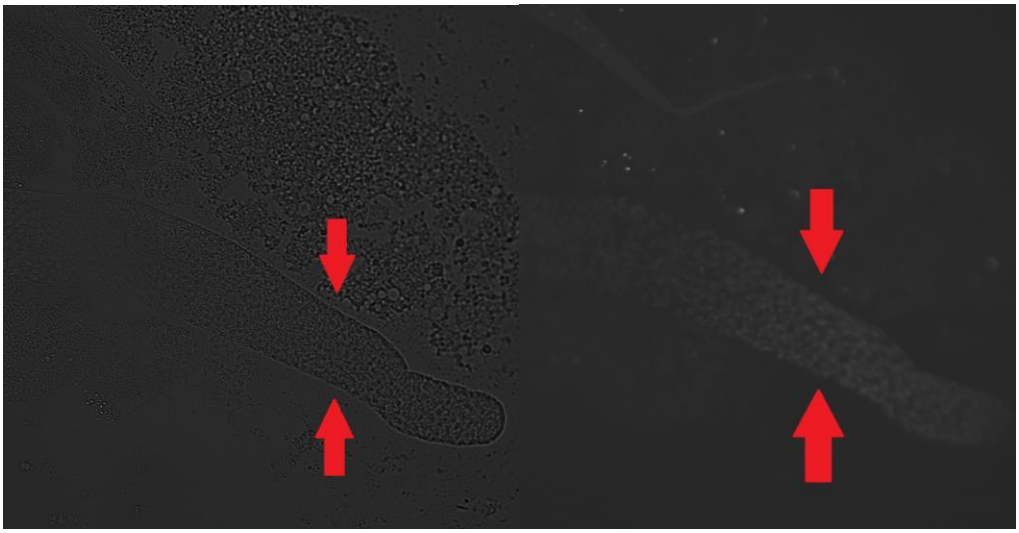

a) b)

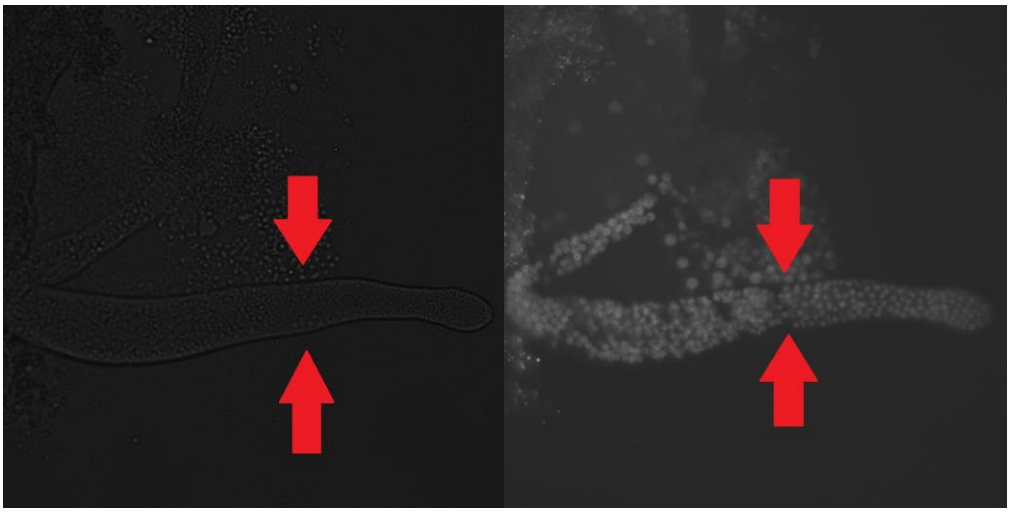

c) d)

Figure 15 *rps-28*p-TIR1 transgenic strain with degron-tagged LIN-35 Fluorescent Imaging 3

Images of auxin-treated *rps-28*p-TIR1 transgenic strain with degron-tagged LIN-35 under normal light (a) and fluorescence (b). Images of vehicle *rps*-28p-TIR1 transgenic strain with degron-tagged LIN-35 under normal light (c) ad fluorescence (d). Germline is indicated by an arrow.

Plate #	Auxin-treated	Vehicle
1	242	310
2	294	367
3	291	295
4	190	306
5	229	320
6	233	306
7	286	269
8	250	318
Average	251.75	311.38
Standard Deviation	36.24	33.3

Table 4 Brood Sizes of *eft-3*p-TIR1 transgenic strain with degron-tagged LIN-35

Table depicting progeny counts of the *eft-3*p-TIR1 transgenic strain with degron-tagged LIN-35.

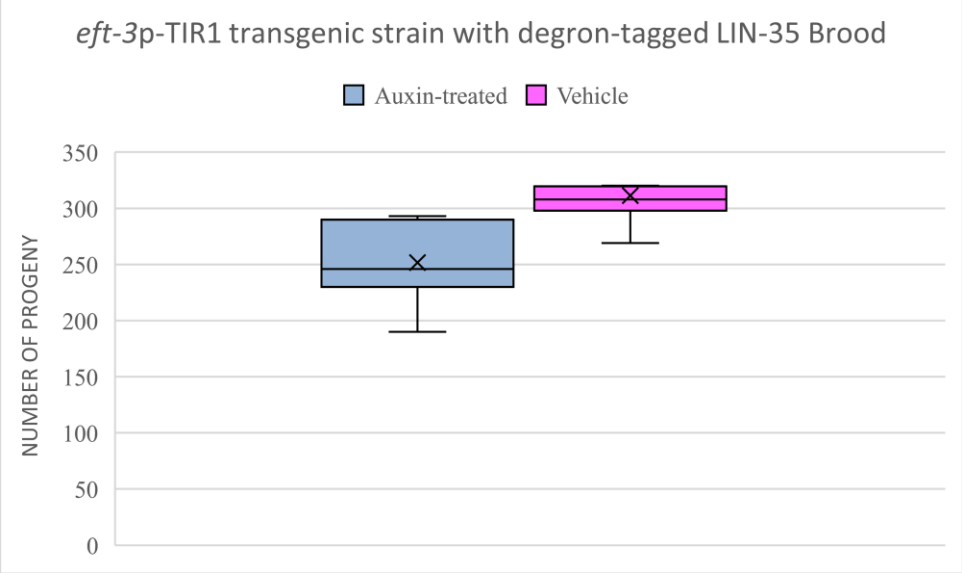

Figure 16 *eft-3*p-TIR1 transgenic strain with degron-tagged LIN-35 brood counting experiment

Box-and-whisker chart comparing the effect of auxin-treatment vs vehicle on progeny count in the *eft-3*p-TIR1 transgenic strain with degron-tagged LIN-35. Significance testing was performed with a two-tailed unpaired T-test. The p-value associated with this data 0.002. A 99% confidence interval was used with $p<0.01$ as the requirement to reject the null hypothesis.

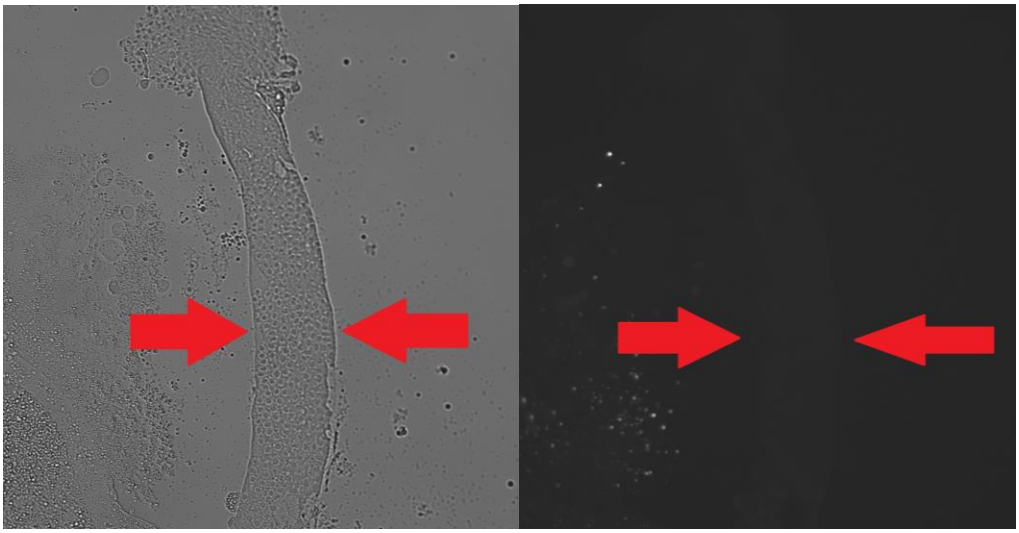

a) b)

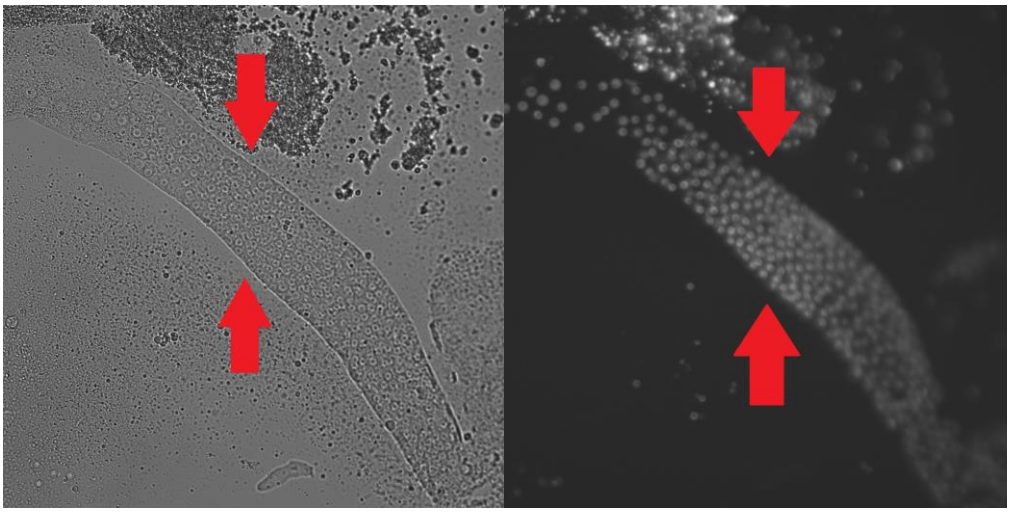

c) d)

Figure 17 *eft-3*p-TIR1 transgenic strain with degron-tagged LIN-35 Fluorescent Imaging 1

Images of auxin-treated *eft-3*p-TIR1 transgenic strain with degron-tagged LIN-35 under normal light (a) and fluorescence (b). Images of vehicle *eft-3*p-TIR1 transgenic strain with degron-tagged LIN-35 under normal light (c) and fluorescence (d). Germline is indicated by an arrow.

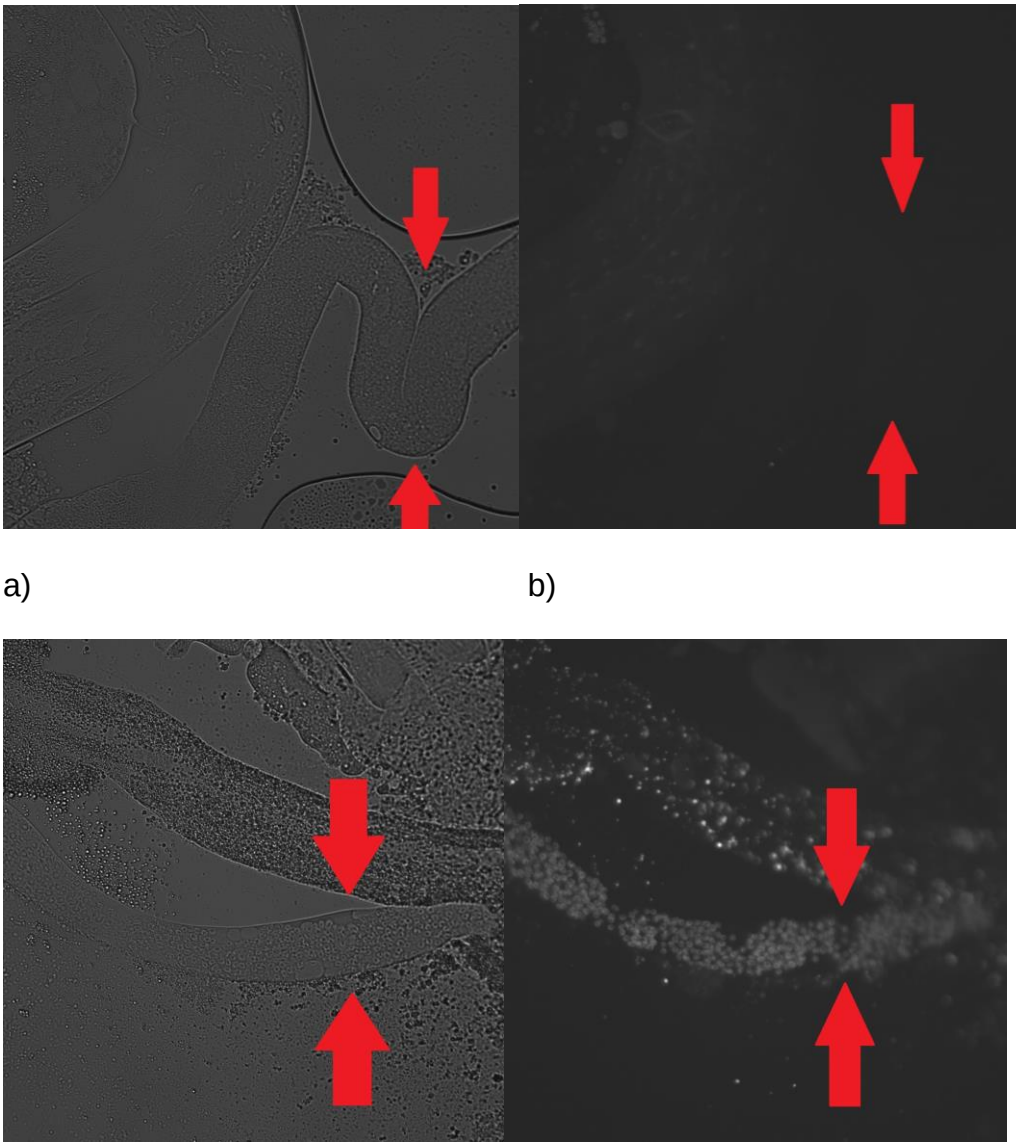

Figure 18 *eft-3*p-TIR1 transgenic strain with degron-tagged LIN-35 Fluorescent Imaging 2

Images of auxin-treated *eft-3*p-TIR1 transgenic strain with degron-tagged LIN-35 under normal light (a) and fluorescence (b). Images of vehicle *eft-3*p-TIR1 transgenic strain with degron-tagged LIN-35 under normal light (c) and fluorescence (d). Germline is indicated by an arrow.

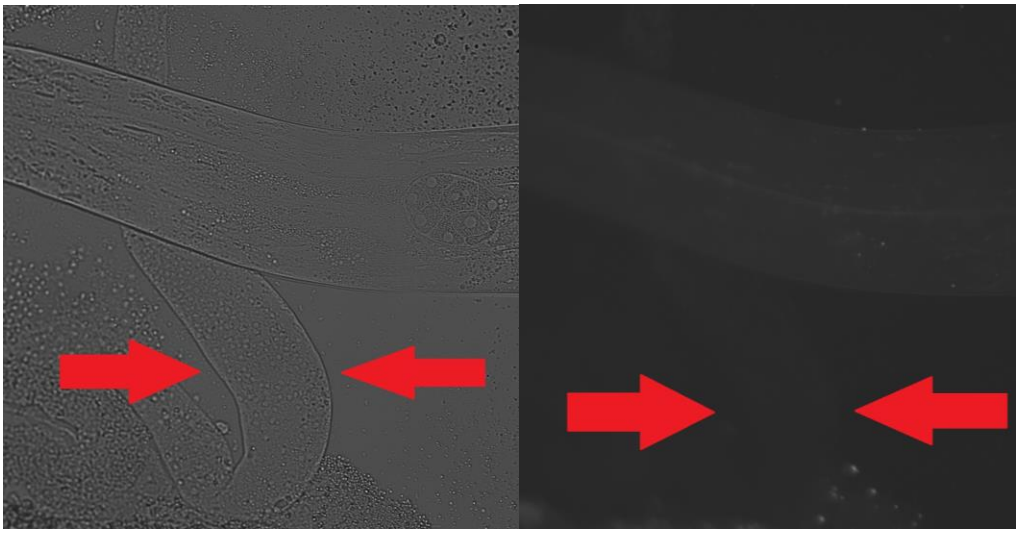

a) b)

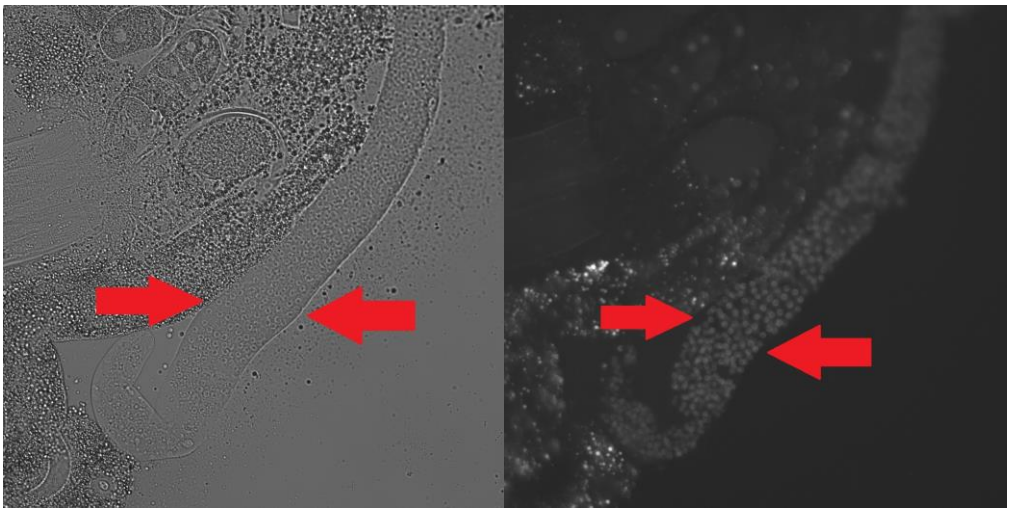

c) d)

Figure 19 *eft-3*p-TIR1 transgenic strain with degron-tagged LIN-35 Fluorescent Imaging 3

Images of auxin-treated *eft-3*p-TIR1 transgenic strain with degron-tagged LIN-35 under normal light (a) and fluorescence (b). Images of vehicle *eft-3*p-TIR1 transgenic strain with degron-tagged LIN-35 under normal light (c) and fluorescence (d). Germline is indicated by an arrow.

1.4 Discussion

The DREAM complex is known to function as a transcriptional repressor of cell-cycle dependent genes. Properly functioning DREAM prevents somatic cells from adopting a germline fate [18]. Disruption of DREAM function leads to ectopic expression of germline genes [19], larval high-temperature arrest [20], and reduced fertility [21]. The knowledge of DREAM functioning to suppress expression of germline genes leads us to wonder the function of DREAM in the germline. This study aimed to fill the gap in knowledge of DREAM function in the germline by evaluating the effects following degradation of LIN-54 or LIN-35 in the germline. LIN-54 is responsible for binding DREAM's MuvB subcomplex to DNA [10,41]. LIN-35 is a pocket protein required for DREAM formation [13,16,42]. Previous studies noted disruption of DREAM in *lin-54* [43] and *lin-35* [16,21] mutant models. A LIN-35 genetic null shows a reduced fertility phenotype [21], while a LIN-54 genetic null is sterile [39]

Our findings suggest that germline degradation of LIN-54 occurred in the presence of auxin. The reduced fertility phenotype observed in the *rps-28*p-TIR1 transgenic strain with degron-tagged LIN-54 supports a previous study that showed LIN-54 is needed to promote germline gene expression in germ cells [43]. Fluorescent imaging showed that there was decreased expression of LIN-54 in both the *rps-28*p-TIR1 transgenic strain with degron-tagged LIN-54 and *eft-3*p-TIR1 transgenic strain with degron-tagged LIN-54. However, the brood sizes of the *eft-3*p-TIR1 transgenic strain with degron-tagged LIN-54 could not be accurately studied due to a high proportion of unexpected worm deaths in the

auxin-treated group. As a result, the cause of the high death-rate in the *eft*-3p-TIR1 transgenic strain with degron-tagged LIN-54 needs to be investigated.

Our LIN-35 findings showed a statistically significant difference in brood size between the auxin-treated and vehicle groups in the *eft-3*p-TIR1 transgenic strain with degron-tagged LIN-35, but not in the *rps-28*p-TIR1 transgenic strain with degron-tagged LIN-35. This suggests that either somatic LIN-35 contributes to fertility, or that somatically-expressed TIR1 was active in the germline. The results of the fluorescent microscopy supports the notion that somatically-expressed TIR1 was active in the germline due to the extensive LIN-35 degradation observed in the germline. Similarly, there was notable degradation of germline LIN-54 in the *eft*-3p-TIR1 transgenic strain with degron-tagged LIN54. However, new TIR1 transgenic strains must be generated to confirm that somatic LIN-54 or LIN-35 does not contribute to fertility.

2 Reference List

1. Wang, Z., Regulation of Cell Cycle Progression by Growth Factor-Induced Cell Signaling. Cells, 2021. 10(12).

2. Carrion, A.M., et al., DREAM is a Ca2+-regulated transcriptional repressor. Nature, 1999. 398(6722): p. 80-4.

3. Schafer, K.A., The cell cycle: a review. Vet Pathol, 1998. 35(6): p. 461-78.

4. Kim, M.J., et al., PAF remodels the DREAM complex to bypass cell quiescence and promote lung tumorigenesis. Mol Cell, 2021. 81(8): p. 1698-1714 e6.

5. Tzachanis, D. and V.A. Boussiotis, Tob, a member of the APRO family, regulates immunological quiescence and tumor suppression. Cell Cycle, 2009. 8(7): p. 1019-25.

6. Kronja, I. and T.L. Orr-Weaver, Translational regulation of the cell cycle: when, where, how and why? Philos Trans R Soc Lond B Biol Sci, 2011. 366(1584): p. 3638-52.

7. Vande Berg, J.S. and M.C. Robson, Arresting cell cycles and the effect on wound healing. Surg Clin North Am, 2003. 83(3): p. 509-20.

8. Frost, E.R., et al., Establishing and maintaining fertility: the importance of cell cycle arrest. Genes Dev, 2021. 35(9-10): p. 619-634.

9. Iness, A.N. and L. Litovchick, MuvB: A Key to Cell Cycle Control in Ovarian Cancer. Front Oncol, 2018. 8: p. 223.

10. Schmit, F., S. Cremer, and S. Gaubatz, LIN54 is an essential core subunit of the DREAM/LINC complex that binds to the cdc2 promoter in a sequence-specific manner. FEBS J, 2009. 276(19): p. 5703-16.

11. Litovchick, L., et al., Evolutionarily conserved multisubunit RBL2/p130 and E2F4 protein complex represses human cell cycle-dependent genes in quiescence. Mol Cell, 2007. 26(4): p. 539-51.

12. Sadasivam, S., S. Duan, and J.A. DeCaprio, The MuvB complex sequentially recruits B-Myb and FoxM1 to promote mitotic gene expression. Genes Dev, 2012. 26(5): p. 474-89.

13. Goetsch, P.D., J.M. Garrigues, and S. Strome, Loss of the Caenorhabditis elegans pocket protein LIN-35 reveals MuvB's innate function as the repressor of DREAM target genes. PLoS Genet, 2017. 13(11): p. e1007088.

14. Kudron, M., et al., Tissue-specific direct targets of Caenorhabditis elegans Rb/E2F dictate distinct somatic and germline programs. Genome Biol, 2013. 14(1): p. R5.

15. Brenner, S., The genetics of Caenorhabditis elegans. Genetics, 1974. 77(1): p. 71-94.

16. Goetsch, P.D. and S. Strome, DREAM interrupted: severing LIN-35-MuvB association in Caenorhabditis elegans impairs DREAM function but not its chromatin localization. Genetics, 2022. 221(3).

17. Vorster, P.J., et al., A long lost key opens an ancient lock: Drosophila Myb causes a synthetic multivulval phenotype in nematodes. Biol Open, 2020. 9(5).

18. Cherian, J.R., K.V. Adams, and L.N. Petrella, Wnt Signaling Drives Ectopic Gene Expression and Larval Arrest in the Absence of the Caenorhabditis elegans DREAM Repressor Complex. G3 (Bethesda), 2020. 10(2): p. 863-874.

19. Wang, D., et al., Somatic misexpression of germline P granules and enhanced RNA interference in retinoblastoma pathway mutants. Nature, 2005. 436(7050): p. 593-7.

20. Petrella, L.N., et al., synMuv B proteins antagonize germline fate in the intestine and ensure C. elegans survival. Development, 2011. 138(6): p. 1069-79.

21. Chi, W. and V. Reinke, Promotion of oogenesis and embryogenesis in the C. elegans gonad by EFL-1/DPL-1 (E2F) does not require LIN-35 (pRB). Development, 2006. 133(16): p. 3147-57.

22. Fire, A., et al., Potent and specific genetic interference by double-stranded RNA in Caenorhabditis elegans. Nature, 1998. 391(6669): p. 806-11.

23. Prozzillo, Y., et al., Targeted Protein Degradation Tools: Overview and Future Perspectives. Biology (Basel), 2020. 9(12).

24. Jackson, A.L., et al., Expression profiling reveals off-target gene regulation by RNAi. Nat Biotechnol, 2003. 21(6): p. 635-7.

25. Rossi, A., et al., Genetic compensation induced by deleterious mutations but not gene knockdowns. Nature, 2015. 524(7564): p. 230-3.

26. Nishimura, K., et al., An auxin-based degron system for the rapid depletion of proteins in nonplant cells. Nat Methods, 2009. 6(12): p. 917-22.

27. Caussinus, E., O. Kanca, and M. Affolter, Fluorescent fusion protein knockout mediated by anti-GFP nanobody. Nat Struct Mol Biol, 2011. 19(1): p. 117-21.

28. Dharmasiri, N., S. Dharmasiri, and M. Estelle, The F-box protein TIR1 is an auxin receptor. Nature, 2005. 435(7041): p. 441-5.

29. Yu, H., et al., Mutations in the TIR1 auxin receptor that increase affinity for auxin/indole-3-acetic acid proteins result in auxin hypersensitivity. Plant Physiol, 2013. 162(1): p. 295-303.

30. Vo, A.A., et al., Efficient generation of a single-copy eft-3p::TIR1::F2A:: BFP::AID*::NLS allele in the C. elegans ttTi5605 insertion site through recombination-mediated cassette exchange. MicroPubl Biol, 2021. 2021.

31. Zhang, L., et al., The auxin-inducible degradation (AID) system enables versatile conditional protein depletion in C. elegans. Development, 2015. 142(24): p. 4374-84.

32. Abel, S. and A. Theologis, Early genes and auxin action. Plant Physiol, 1996. 111(1): p. 9-17.

33. Natsume, T., et al., Rapid Protein Depletion in Human Cells by Auxin-Inducible Degron Tagging with Short Homology Donors. Cell Rep, 2016. 15(1): p. 210-218.

34. Schiksnis, E., et al., Auxin-independent depletion of degron-tagged proteins by TIR1. MicroPubl Biol, 2020. 2020.

35. Martinez, M.A.Q., et al., Rapid Degradation of Caenorhabditis elegans Proteins at Single-Cell Resolution with a Synthetic Auxin. G3 (Bethesda), 2020. 10(1): p. 267-280.

36. Negishi, T., et al., The auxin-inducible degron 2 (AID2) system enables controlled protein knockdown during embryogenesis and development in Caenorhabditis elegans. Genetics, 2022. 220(2).

37. Loose, J.A. and A. Ghazi, Auxin treatment increases lifespan in Caenorhabditis elegans. Biol Open, 2021. 10(5).

38. Yesbolatova, A., et al., The auxin-inducible degron 2 technology provides sharp degradation control in yeast, mammalian cells, and mice. Nat Commun, 2020. 11(1): p. 5701.

39. Tabuchi, T.M., et al., Opposing activities of DRM and MES-4 tune gene expression and X-chromosome repression in Caenorhabditis elegans germ cells. G3 (Bethesda), 2014. 4(1): p. 143-53.

40. Edelstein, A.D., et al., Advanced methods of microscope control using muManager software. J Biol Methods, 2014. 1(2).

41. Muller, G.A., et al., The CHR site: definition and genome-wide identification of a cell cycle transcriptional element. Nucleic Acids Res, 2014. 42(16): p. 10331-50.

42. Kirienko, N.V. and D.S. Fay, Transcriptome profiling of the C. elegans Rb ortholog reveals diverse developmental roles. Dev Biol, 2007. 305(2): p. 674-84.

43. Tabuchi, T.M., et al., Chromosome-biased binding and gene regulation by the Caenorhabditis elegans DRM complex. PLoS Genet, 2011. 7(5): p. e1002074.